Rogers, J. W., B. A. Hagenhoff, A. E. Cohen, R. L Thompson, B. T. Smith, and E. E. Carpenter, 2016: Lower Mississippi River Valley quasi-linear convective system tornado environments and radar signatures. *J. Operational Meteor.*, **5** (4), 42-52, doi: https://doi.org/10.15191/nwajom.2017.0504.

Lower Mississippi River Valley Quasi-Linear Convective System Tornado Environments and Radar Signatures

JARET W. ROGERS
NOAA/NWS/NCEP/Storm Prediction Center, Norman, Oklahoma

BROOKE A. HAGENHOFF
University of North Dakota, Grand Forks, North Dakota

ARIEL E. COHEN, RICHARD L. THOMPSON, BRYAN T.SMITH
NOAA/NWS/NCEP/Storm Prediction Center, Norman, Oklahoma

ERIC E. CARPENTER
NOAA/NWS, Jackson, Mississippi

(Manuscript received 11 August 2016; review completed 21 November 2016)

ABSTRACT

Considerable research has compared quasi-linear convective system (QLCS) tornadoes and tornadoes associated with other convective modes. The present study seeks to identify environmental and radar characteristics associated with, specifically, QLCS tornadoes occurring in the lower Mississippi River Valley, with analysis focused on seasonal and tornado-intensity variability. Archived radar and mesoanalysis data from 2009–2013 are analyzed to identify the environmental and storm-scale characteristics associated with lower Mississippi Valley tornadoes, and a comparison is made with both QLCS and non-QLCS tornadoes across the remainder of the United States to identify unique attributes. Analysis of the environmental variables in this regime suggests relatively lower magnitudes of lowest 100-hPa mean-layer convective available potential energy (CAPE) when compared to all other tornadoes (non-QLCS modes in the lower Mississippi Valley and all modes in all other portions of the United States). However, the low-level and deep-layer bulk wind differences for lower Mississippi River Valley QLCS tornadic storms are similar to other tornadic storms. Although previous studies often noted the relationship between CAPE and tornado potential, significant QLCS tornadoes are found to occur in low CAPE environments. Additionally, radar data from a sample of the QLCS tornadoes from the dataset were examined, considering the rotational velocity up to three radar volume scans before the initial tornado report to determine characteristics of radar circulations associated with QLCS tornadoes prior to their occurrence. Temporal trends in rotational velocity are provided and could serve as guidance to forecasters in anticipating QLCS tornado occurrence in a short-term forecast scenario.

1. Introduction

Quasi-linear convective system (QLCS) tornadoes pose substantial challenges to operational forecasters owing to their rapid development and detection difficulties related to radar sampling limitations. The development of QLCSs during the cool season months (i.e., November through March) is often associated with synoptically evident mid- and upper-level troughs supporting strong forcing for ascent (e.g., Browning 1986; Branick et al. 1988). Environments supporting severe thunderstorms are known to accompany many of these synoptic-scale mid- and upper-level troughs, but identifying tornado potential within these broader environments remains a challenge.

The lower Mississippi Valley (LMV) of the United States, located within a relative spatial maximum in tornado activity referred to as Dixie Tornado Alley (Gagan et al. 2010), has experienced tornadoes at all times of year. Previous research shows that most

Corresponding author address: Jaret W. Rogers, NOAA/NWS/NCEP/Storm Prediction Center, Ste. 2300, 120 David L. Boren Blvd., Norman, OK 73072
E-mail: jaret.rogers@noaa.gov

tornadoes that occur from November through March across the LMV are nocturnal in nature (Smith et al. 2012, hereafter S12), further complicating efforts to receive ground-truth by operational forecasters and posing concerns regarding warning preparedness for the general population in an area where tornado fatalities are common (Ashley 2007).

As shown by S12, most QLCS tornadoes occur east of the Great Plains, with a spatial maximum focused in the Ohio and Mississippi valleys (Trapp et al. 2005; Thompson et al. 2013). Thompson et al. (2012, hereafter T12) confirm that QLCS tornado environments exhibit stronger vertical shear and weaker buoyancy compared to the large buoyancy and steeper midlevel lapse rates characteristic of Great Plains tornado environments. The near-storm environment for QLCS tornadoes is often characterized by the lowest 100-hPa mean-layer convective available potential energy (MLCAPE) <1000 J/kg^{-1}, and the lowest 100-hPa mean-layer lifting condensation level heights are rarely above 1000 m (Thompson et al. 2013). One prominent QLCS tornado outbreak case featuring similar environmental conditions occurred on 31 October 2013 and was analyzed in detail by Guyer and Jirak (2014). The occurrence of QLCS tornadoes in this case was consistent with findings presented by Thompson et al. (2013) and highlights the incidence of tornadoes in environments featuring very strong 0–6 km bulk wind difference (BWD) magnitudes (i.e., ≥25 m/s^{-1}) but limited buoyancy (i.e., MLCAPE ≤1000 J/kg^{-1}).

Most QLCS tornadoes are weak in nature, with S12 showing that nearly 89% of events are associated with an Enhanced Fujita (EF) rating of EF0 or EF1. Guyer and Dean (2010) find that tornadoes occurring in environments characterized by weak MLCAPE (≤500 J/kg^{-1}) frequently occur overnight and are most common during the winter and spring/fall transition months. However, strong tornadoes can occasionally occur within a QLCS. One such example features two separate EF3 tornadoes occurring within a QLCS over central Alabama at 0944 and 1018 UTC on 27 April 2011. A comprehensive study of QLCS tornado events by S12 found 11 EF3 or stronger QLCS tornadoes occurred between 2003 and 2011 across the contiguous United States (CONUS), and these events occurred in an environmental parameter space supportive of supercells (T12).

Previous research related to QLCS environments and tornadoes primarily have been regional in scope within the United States, including an extensive study documenting QLCS tornadoes in the middle Mississippi valley (e.g., Przybylinski et al. 2013). A radar climatology of tornadic and nontornadic vortices in high-shear, low CAPE environments in the Southeast and mid-Atlantic (e.g., Davis and Parker 2014) included a large subset of QLCS events. However, no known formal study exists that focuses solely on LMV QLCS tornado environments. The goal of the present study is to provide an overview of environmental and radar-based characteristics of QLCS tornadoes occurring in the LMV to assist operational forecasters in contextualizing environments conducive for tornadoes relative to other tornado regimes. This work represents an attempt to understand the specific LMV QLCS tornado regime as a separate spatial and convective-mode entity, building upon the work from previous studies. Additional analyses investigate how these characteristics compare to all other tornadoes (all regions and modes) in an effort to determine characteristics that make LMV QLCS tornado environments and radar attributes distinguishable.

2. Data and Methods

The present study uses work detailed by S12, T12, and Thompson et al. (2013) as the foundation for analysis of the mesoscale environment characteristic of tornadoes. This foundation interweaves the relationship between tornadoes and their associated convective mode with thermodynamic and kinematic parameters representative of the environment, using data from the Storm Prediction Center mesoanalysis system (Bothwell et al. 2002). Such work permits analysis of tornado environments specifically associated with the QLCS convective mode and within the specific region of the LMV.

The initial locations corresponding to QLCS tornadoes relevant for further analysis are provided in Fig. 1. This area lies south of 36.0°N and between 94.5°W and 88.0°W and extends through the period of 2009–2013, which corresponds with the availability of Level II super-resolution radar data. Analyses of thermodynamic parameters (e.g., CAPE, lapse rate, dewpoint, and precipitable water), along with kinematic parameters [e.g., storm-relative helicity (SRH) and BWD], are based upon these events featured in Fig. 1. Variability associated with these parameters for QLCS tornadoes is examined seasonally and by EF-scale intensity to investigate parameter magnitude variations between different times of year and different tornado damage magnitudes.

Environmental data obtained from the Storm

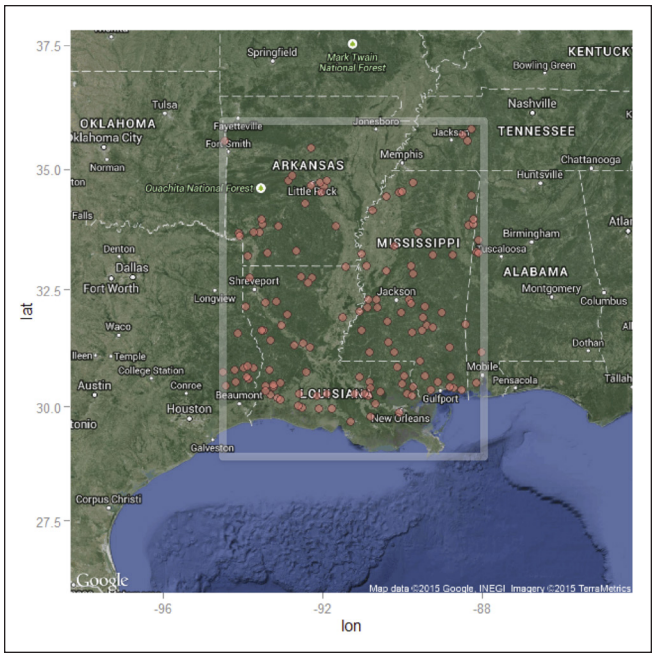

Figure 1. QLCS tornado events using the documented starting latitude/longitude points along with an outline of the domain of interest (in semi-transparent-white rectangle) corresponding to the LMV. *Click image for an external version; this applies to all figures hereafter.*

Prediction Center (SPC) mesoanalysis system (Bothwell et al. 2002) are matched with the tornadoes shown in Fig. 1 and then plotted per EF-scale magnitude and season. Furthermore, an analysis of CAPE, wind shear, and moisture parameters commonly used to diagnose severe weather potential is performed to identify favorable environmental and radar characteristics for QLCS tornado events. Environmental conditions corresponding to tornadoes are based on thermodynamic and kinematic profiles at the nearest grid point, rather than interpolation to tornado locations.

Sources of error inherent to the SPC mesoanalysis system ultimately influence the validity of the environment characterizing the tornadoes compared to the true atmosphere. For instance, inaccuracies in vertical profiles above the ground, driven to some extent by planetary boundary layer parameterization schemes with known flaws (Cohen et al. 2015), can extend to the mesoanalysis output. These errors may become important in low-buoyancy environments where relatively small variations in depicted instability measures can offer substantially varying implications regarding convective impacts. Cohen et al. (2015) address additional details related to these sources of error, especially in the realm of southeastern United States cold-season severe weather environments. Furthermore, instrumentation error and smoothing of analysis fields manifested in the SPC mesoanalysis output could serve as error sources in describing the near-storm environment. Where sharp spatial gradients in analyzed parameters exist, it is possible for the nearest grid point environmental characteristics to inadequately describe the true near-storm environment. These are all relevant sources of error for subsequent analysis. Regardless, the SPC mesoanalysis system has proven reproducibly to offer invaluable insight regarding the convective environment and related hazards and is treated within the meteorological community as the primary means for real-time, mesoscale environmental assessment.

Furthermore, the database also includes information regarding radar attributes of the low-level circulations attendant to the tornadoes, including rotational velocity trends and convective mode. Additional details regarding the documentation of these attributes and their applications are available from S12, T12, and Smith et al. (2015, hereafter S15). This study analyzed radar attributes for LMV QLCS tornadoes (Fig. 1). Specific radar attributes examined include: 1) peak rotational velocity, 2) distance between maximum inbound and outbound radial velocities within the storm-scale circulation, and 3) distance from radar and height above radar level (e.g., ≤3 km). The purpose of this work is to provide guidance regarding typical velocity data associated with QLCS tornadoes. However, this work includes an additional component beyond that available in the SPC convective mode and environment database by examining temporal trends in pre-QLCS-tornado peak rotational velocity for a subset of tornado cases to illustrate storm-scale circulation evolution prior to tornado occurrence.

Environmental and radar data obtained from the SPC mesoanalysis system (Bothwell et al. 2002) are matched with the tornadoes shown in Fig. 1 and then plotted by EF-scale magnitude and season. An analysis of CAPE, wind shear, and moisture parameters commonly used to diagnose severe weather potential is performed to identify favorable environmental and radar characteristics for QLCS tornado events. The radar analyses focus on rotational velocity and azimuthal shear trends leading up to the tornadoes.

A total of 138 QLCS tornadoes were identified within the LMV between 2009 and 2013. Annual observed totals ranged from a minimum of 3 cases in 2010 to a maximum of 45 cases in 2011.

3. Results

a. Comparison of environmental parameters separated by EF-scale rating

The distribution of LMV QLCS tornadoes by EF-scale rating in the present study includes 46 EF0, 78 EF1, 14 EF2 cases, and no tornadoes rated higher than EF2. Owing to the limited sample size of tornadoes rated EF2, comparisons of EF-scale ratings throughout the remainder of the paper will focus on EF0 tornadoes with EF1 and EF2 tornadoes (hereafter, referred to as EF1+). This approach is similar to S15, which grouped EF2 and stronger QLCS tornadoes together due to a limited sample size of higher EF-scale ratings.

Past literature has focused on the positive correlation between thermodynamic indices (e.g., MLCAPE) and EF-scale rating, especially for tornadoes occurring within right-moving supercells (T12; S15, their Fig. 9). This relationship is much weaker when considering environments of QLCS tornadoes, and higher MLCAPE values do not necessarily correspond to increased potential for significant tornadoes (T12, their Fig. 5). In fact, T12 found that the mean MLCAPE value associated with a large sample of EF2 QLCS tornadoes across the CONUS was slightly less than the value for EF0 QLCS tornadoes.

The current study demonstrates a slight positive relationship between the distribution of MLCAPE values and EF-scale rating for LMV QLCS tornadoes, as shown in Fig. 2a. Most notably, the mean MLCAPE value is approximately 200 J/kg^{-1} higher for EF1+ tornadoes. Outliers featuring MLCAPE values >2000 J/kg^{-1} are usually associated with EF1+ tornadoes. However, little discrimination in the magnitude distributions of each EF-scale group is noted, suggesting that MLCAPE remains a poor discriminator of EF-scale rating. Virtually no difference in the parameter distribution of 0–3 km above ground level (AGL) MLCAPE is found (Fig. 2b).

Kinematic parameters commonly used to characterize severe storm environments, including effective-layer BWD and SRH, exhibit a slight increase in magnitude in conjunction with higher EF-scale ratings, with results being fairly consistent with T12. Mean effective BWD values (Fig. 2c) are slightly lower for EF0 tornadoes (22 m/s^{-1}; 43 kt) than for EF1+ tornadoes (25.3 m/s^{-1}; 49 kt). It should be noted that the calculation of SRH values within the effective layer assumes a mean storm motion associated with right-moving supercells. However, effective SRH is a component in the calculation of the effective-layer significant tornado parameter, and this parameter for LMV QLCS tornadoes is analyzed to provide a consistent comparison with results from T12 and Thompson et al. (2013). Mean effective SRH values (Fig. 2d) exhibit an increase between EF0 ratings (216 m2 s–2) and EF1+ ratings (264 m2 s–2). Kinematic parameters defined by a fixed layer exhibit negligible differences in the mean values and overall distribution between EF0 ratings and EF1+ ratings for both 0–3-km bulk wind shear (Fig. 2e) and 0–3-km SRH (Fig. 2f). Of note, the entire box plot representing 0–3-km bulk wind shear magnitudes for both EF0 and EF1+ ratings are >30 kt, which is consistent with a favorable 0–3-km line-normal bulk shear magnitude threshold identified by Schaumann and Przybylinski (2012) for QLCS tornado-producing mesovortices. Substantial overlap in the parameter distributions for effective BWD and effective SRH suggest that commonly used parameters for characterizing both the kinematic and thermodynamic environment are poor discriminators of EF-scale rating, despite exhibiting a slight positive relationship with increasing EF-scale rating.

b. Spatiotemporal characteristics of QLCS tornadoes

The hourly distribution of LMV QLCS tornado occurrence does not exhibit a distinct peak (Fig. 3a) and is similar to diurnal frequency trends examined within a longer period by S12 (their Fig. 24) for QLCS tornadoes occurring within 200 km of Jackson, Mississippi. Nocturnal tornadoes are more frequently associated with QLCS events than non-QLCS events, which exhibit a distinct diurnal trend featuring a peak in the late afternoon and early evening hours (Fig. 3b). Hart and Cohen (2016a) explore within-year variability of convective parameters relevant for significant tornado forecasting, and they identify differences in the predictability of significant tornadoes from November through May (more predictability) and June through October (less predictability) using the Statistical Severe Convective Risk Assessment Model for convective parameters introduced by Hart and Cohen (2016b). The present study seeks to provide additional insight regarding the behavior of seasonal variability for meteorological parameters characterizing a relatively small subset of the tornado database.

QLCS tornadoes are almost entirely confined to the winter and spring/fall transition months across the LMV, exhibit a distinct peak in March and April (Fig. 4), and are infrequent during meteorological

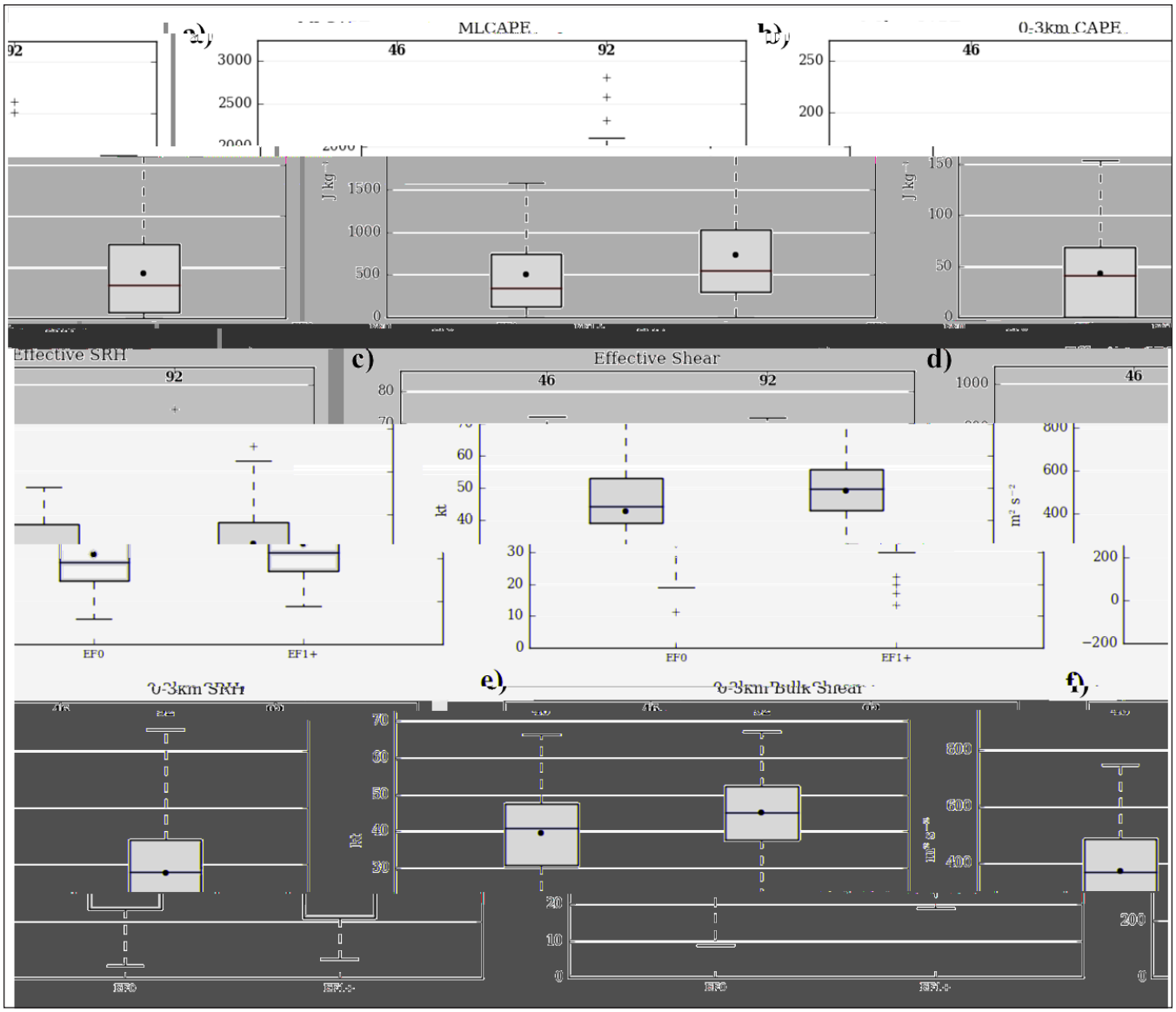

Figure 2. Box-and-whisker plots of (a) MLCAPE, (b) 0–3 km CAPE, (c) effective BWD, (d) effective SRH, (e) 0–3 km bulk shear, and (f) 0–3 km SRH for LMV QLCS tornadoes for EF0 and EF1+ ratings. Each box-and-whisker plot is composed of a median value (bold black line), mean (black dot), interquartile range (IQR) 25%–75% (box), and whiskers extending to 1.5 times the IQR beyond the IQR. The sample size is shown above each box in bold black font.

summer (June–August). A comparison of environments during the seasons most favorable for LMV QLCS tornadoes classified by meteorological fall (September–November), winter (December–February), and spring (March–May) reveals notable differences amongst several thermodynamic parameters. One caveat in the seasonal comparisons is the relatively small sample size of tornadoes occurring in the fall, featuring only 15 cases, whereas 42 and 77 cases occurred in the winter and spring, respectively. Parameters characterizing the degree of buoyancy show a minimum in winter for MLCAPE (Fig. 5a), exhibiting a mean value approximately 120–200 J/kg^{-1} lower than fall and spring. All three seasons exhibit outlier events where MLCAPE is <100 J/kg^{-1}, suggesting large MLCAPE values are not necessary for QLCS tornadoes to occur in every case. A similar observation is noted in T12, in which a large majority of winter QLCS tornado cases across the CONUS occurred with MLCAPE values <400 J/kg^{-1}. However, the distribution of winter MLCAPE values amongst LMV QLCS tornado cases observed in the present study features a larger interquartile range

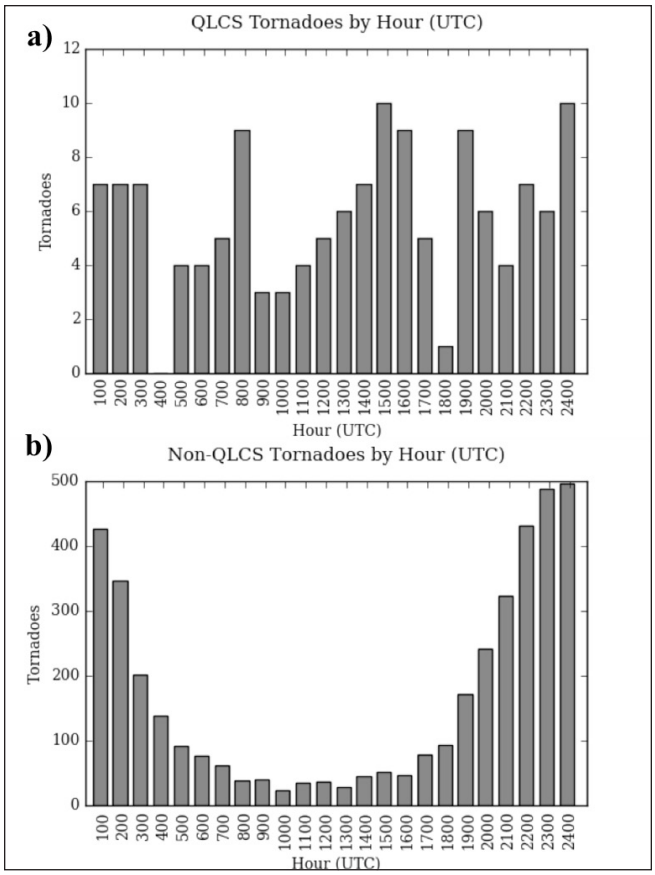

Figure 3. a) LMV QLCS tornadoes and b) non-QLCS tornadoes for the contiguous United States, binned by hour (UTC) of the initial tornado report.

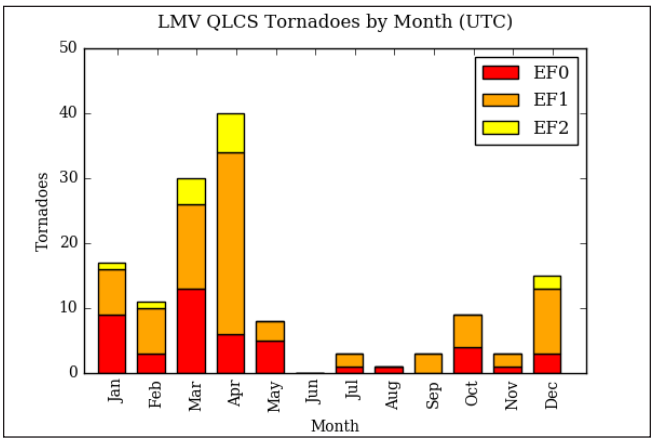

Figure 4. Number of LMV QLCS tornadoes by month, separated by EF-scale rating.

(Fig. 5a) compared to T12, with a magnitude near 800 J/kg^{-1} at the top of the interquartile range. This suggests that winter environments favorable for LMV QLCS tornadoes may occasionally exhibit greater buoyancy than what occurs in other parts of the country. MLCAPE values in the lowest 0–3-km AGL show a gradual decrease in the mean and median values from fall into winter and spring (Fig. 5b), but substantial overlap in the distributions is noted.

The distributions of lapse rates show a tendency for higher values in the winter and spring, especially in the midlevels of the troposphere. Lapse rates within the 0–3-km layer AGL (Fig. 5c) are slightly weaker in the fall than winter and spring, exhibiting a mean and median value smaller by approximately 0.3°C km^{-1}, whereas both winter and spring are nearly identical in magnitude and overall distribution. More notable differences exist within the 700–500 hPa layer (Fig. 5d), with mean and median values approximately 0.5–1.0°C lower in the fall compared to winter and spring.

Moisture parameters exhibit distinct seasonal differences, following typical variations across the region. Most commonly, QLCS tornadoes in the fall occur in environments featuring rich tropospheric moisture, as noted by a mean precipitable water (PW) value of 53 mm (2.1 in; Fig. 5e). In contrast, the median PW values on 15 October for Jackson, Mississippi (JAN), and Slidell, Louisiana (LIX), are between 25.4 mm and 33.0 (1.0–1.3 in), per SPC's sounding climatology database (Rogers et al. 2014). Winter and spring QLCS tornadoes occur within environments that can be characterized as seasonably moist, featuring mean PW values of 40.6 to 43.2 mm (1.6 to 1.7 in), but still much lower in magnitude than what occurs in fall. Median PW values for observed soundings at JAN and LIX generally range between 12.7 mm and 25.4 mm (0.5–1.0 in) for much of the winter through the middle of spring.

c. Comparison of LMV QLCS tornadoes to remainder of tornadoes across the CONUS

QLCS tornadoes across the LMV are compared with tornadoes elsewhere across the CONUS, including all other convective modes, to determine differences in commonly observed environmental parameters. MLCAPE (Fig. 6a) exhibits a notable difference between LMV QLCS tornadoes and all other tornadoes, with mean values 800 J/kg^{-1} and 400 J/kg^{-1} lower for EF0 and EF1+ ratings, respectively. These comparisons are fairly consistent with T12, which found a mean MLCAPE difference of 638 J/kg^{-1} between QLCS EF0 and discrete right-moving supercell EF0 tornadoes. T12 found a weak inverse relationship between EF-scale rating and MLCAPE magnitude for QLCS tornadoes across the CONUS, featuring median values of 1112

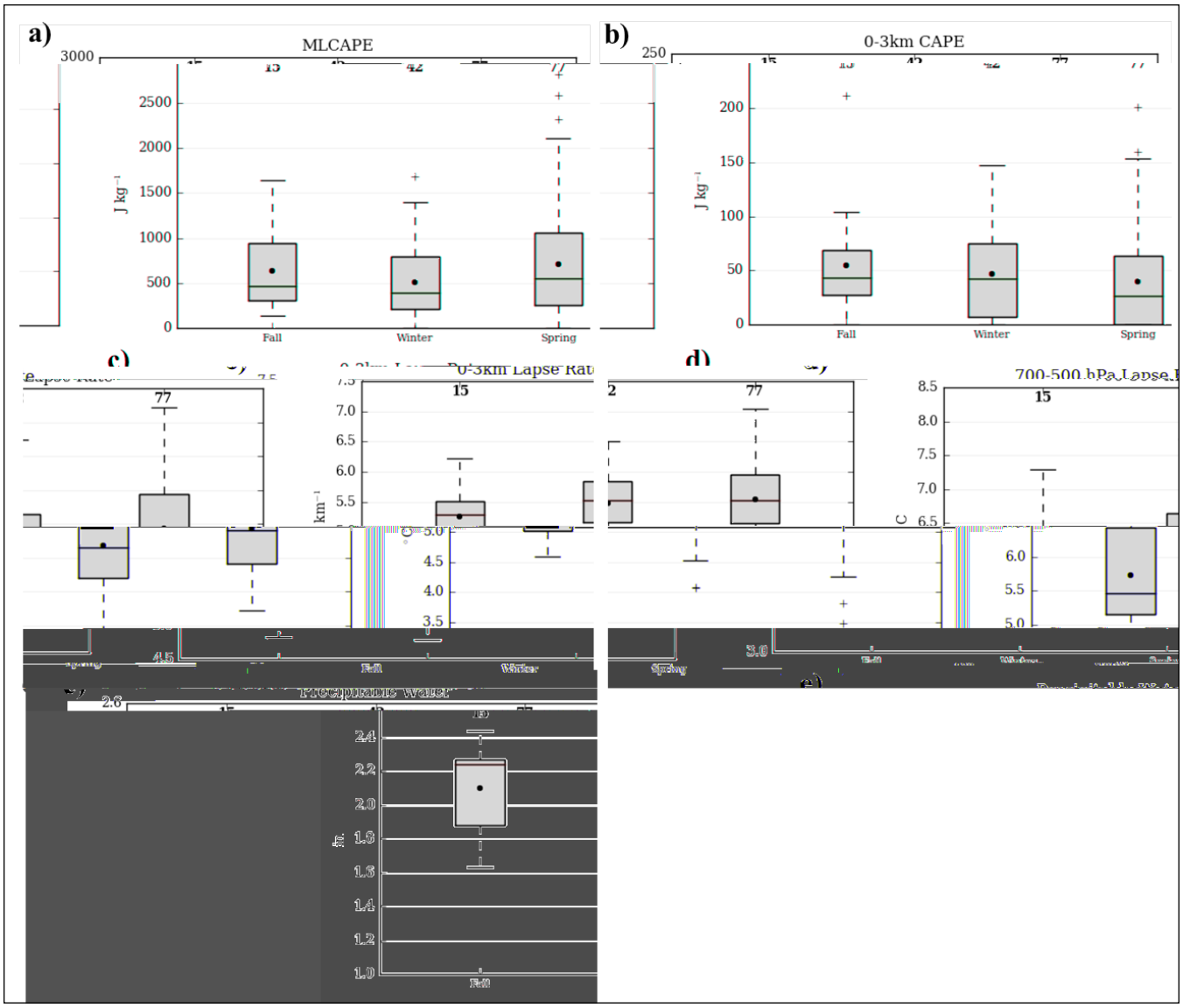

Figure 5. Box-and-whisker plots depicting the distribution of (a) MLCAPE, (b) 0–3 km layer CAPE, (c) 0–3 km layer AGL lapse rates, (d) 700–500 hPa layer lapse rates, and (e) precipitable water for LMV QLCS tornadoes. Seasons are designated by the meteorological definition of fall (September–November), winter (December–February), and spring (March–May). Box-and-whisker plot conventions follow those described in Fig. 2.

J/kg^{-1} for nontornadic cases, 680 J/kg^{-1} for EF0 cases, and 587 J/kg^{-1} for EF1+ cases. This finding differs from LMV cases analyzed in the present study, which found similar distributions of MLCAPE values for both EF0 and EF1+ cases (Fig. 6a). MLCAPE values in the lowest 0–3-km AGL layer (Fig. 6b) also exhibit generally lower values within the distribution of LMV QLCS tornadoes compared with all other tornadoes.

A similar comparison of kinematic parameters reveals negligible differences between LMV QLCS tornadoes and those in the rest of the CONUS. Both the mean and median values of effective BWD (Fig. 6c) are similar for EF0 and EF1+ ratings for LMV QLCS tornadoes. The only notable difference in the distribution is the lower extension of the box-and-whisker plot in Fig. 6c for EF0 tornadoes across the CONUS, which encompasses environments featuring lower magnitudes of effective BWD than what are observed with LMV QLCS tornadoes. Similar distributions also are noted when comparing effective SRH (Fig. 6d). Larger differences in kinematic parameters associated with QLCS and right-moving supercells were noted in T12, with mean effective BWD values differing by 3.6 m/s^{-1} (7 kt) for EF0 tornadoes and 5.1 m/s^{-1} (10 kt)

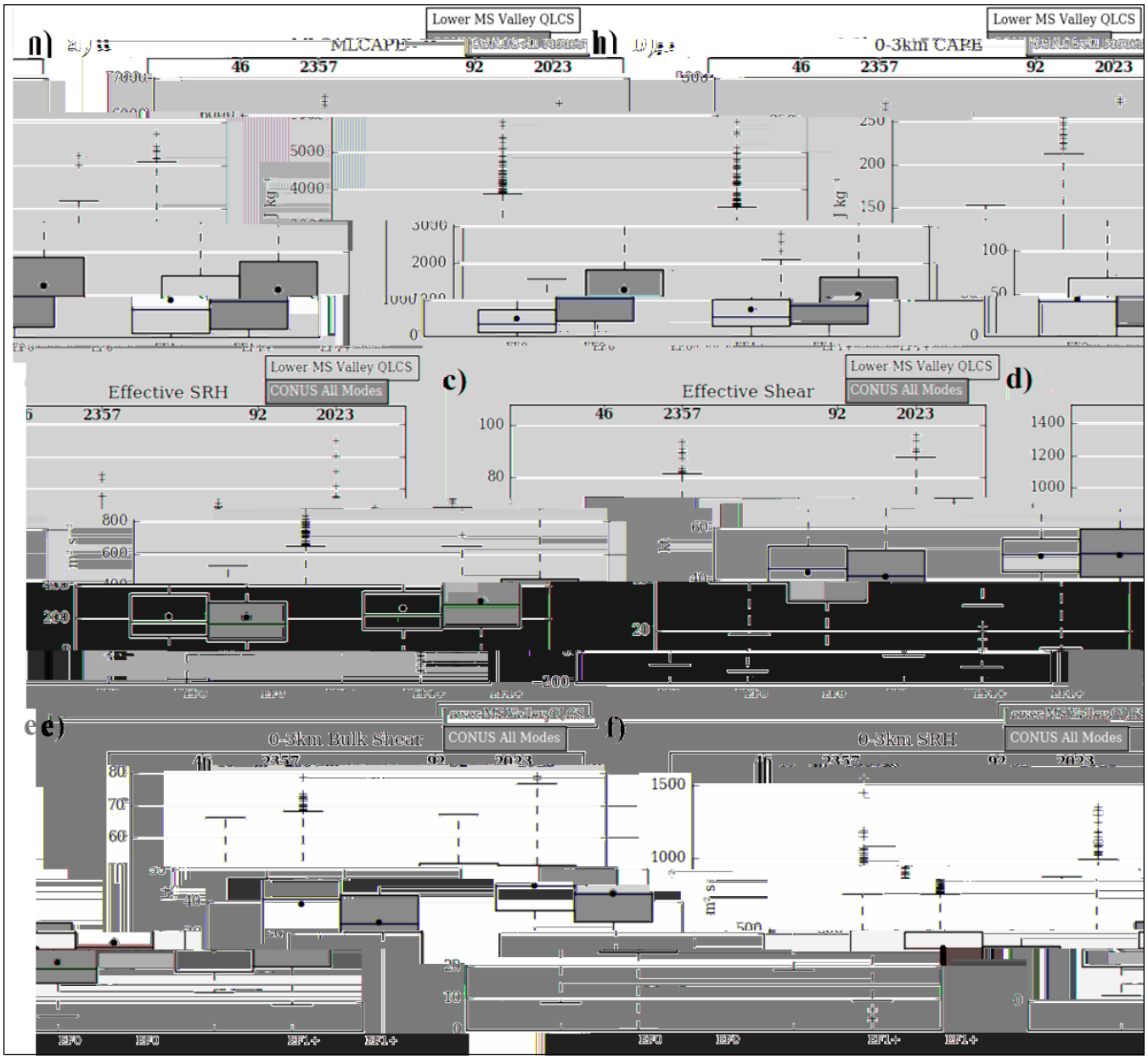

Figure 6. Box-and-whisker plots depicting the distribution of (a) MLCAPE, (b) 0–3 km layer AGL CAPE, (c) effective BWD, and (d) effective SRH, (e) 0–3 km bulk shear, and (f) 0–3 km SRH for QLCS tornadoes across the LMV (white boxes), and all modes across the remainder of the CONUS and non-QLCS LMV tornadoes (grey boxes) for various EF-scale ratings from 2009–2013. Box-and-whisker plot conventions follow those described in Fig. 2.

for EF2 tornadoes. Fixed-layer kinematic parameter calculations, including 0–3-km bulk wind shear (Fig. 6e) and 0–3-km SRH (Fig. 6f), showed more notable differences in the box plots for EF0 ratings between LMV QLCS cases and all other tornado reports. This is consistent with the notion that many LMV QLCS tornadoes form within environments characterized by high shear and low CAPE, relative to typical tornadic supercell environments across the Plains (T12).

d. Radar Analysis

Rotational velocity trends for varying EF-scale ratings associated with LMV QLCS tornadoes are consistent with CONUS-wide results from S15. Specifically, the peak 0.5° rotational velocity at any

point during the life cycle of the tornado generally increases from tornado ratings of EF0 through EF1+ (Fig. 7a), featuring a mean value of 15.9 m/s^{-1} (31 kt) and 18 m/s^{-1} (35 kt), respectively. The distance between the maximum radial inbound and outbound velocities exhibits a small mean difference of 0.28 km (0.15 n mi) between EF0 and EF1+ tornadoes (Fig. 7b). A subset of EF1+ LMV QLCS tornadoes feature smaller distances between peak inbound and outbound radial velocities, but the overall distribution remains very similar to EF0 tornadoes.

The final component of this study involves individually calculating rotational velocity and the distance between maximum inbound and outbound velocities corresponding to QLCS tornado events prior to tornadogenesis. A small-sample-size subset of the total QLCS tornado events is used to provide a preliminary investigation regarding temporal variability in rotational velocity. Although a much larger sample size would be desirable to gain more confidence in the implied meaning of the results and their physical implications, this manuscript is intended to provide an initial, proof-of-concept approach toward this analysis. This sample subset was restricted in size to an arbitrary number of 29 cases, owing to the appreciable amount of manual labor required for radar analysis. Consequently, this is only a preliminary investigation of circulation trends. Twenty-nine individual cases were selected for analysis based on the adequate data quality and sampling availability.

A temporal analysis of rotational velocity trends from three scans (~11–15 min) to one scan (~1–5 min) prior to the tornado report reveals a gradual increase in magnitude (Fig. 8a). Both mean and median values increase from approximately 14.9 m/s^{-1} (29 kt) to more than 16.5 m/s^{-1} (32 kt) during this period, with a slight corresponding upward shift in the overall distribution of magnitudes also observed. The distance between the maximum inbound and outbound velocities exhibits an inverse trend compared to Fig. 8a, decreasing approximately 0.5 km, on average, from three scans to one scan prior to the tornado report (Fig. 8b). It is noted that these results are based on a relatively small sample size, reducing their overall representativeness of the larger corresponding populations. Davis and Parker (2014; see Fig. 5) noted a similar trend in the temporal change in azimuthal shear magnitude, calculated as the difference in maximum and magnitude of radial velocity divided by distance between the two radar bins for high-shear, low-CAPE environment tornadic cases in the Southeast and mid-Atlantic regions. At the 0.5° elevation scan, a general upward trend in azimuthal shear magnitude from 20 min prior to up until the time of tornado warning issuance by the local National Weather Service forecast office was noted, followed by a decrease to pre-warning magnitudes.

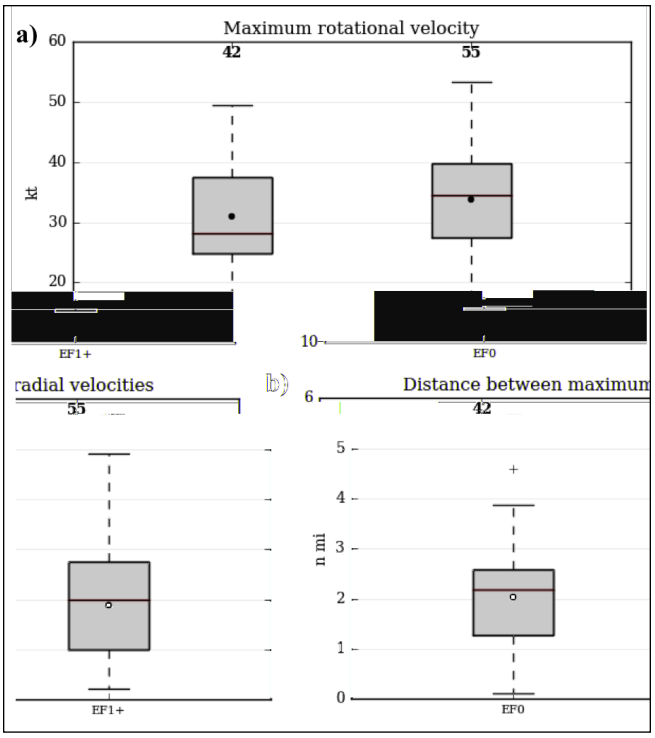

Figure 7. (a) The maximum rotational velocity during the life cycle of the tornado and (b) the distance between the maximum inbound and outbound radial velocities for LMV QLCS tornadoes at varying EF-scale ratings. Box-and-whisker plot conventions follow those described in Fig. 2.

4. Summary and Conclusions

Analyses of mesoscale environment parameters for LMV QLCS tornadoes suggest that these tornadoes tend to form in low-CAPE environments when compared to all other storm modes and regions. Low-CAPE environments of QLCS tornadoes in the LMV tend to occur in environments featuring BWD magnitudes similar to other parts of the country and may compensate for the limited degree of buoyancy. The results presented in the current study are consistent with findings from S12, T12, and S15, which highlight typical environmental and climatological characteristics of QLCS tornadoes across the CONUS.

QLCS tornadoes are found to be most common from October through May, with a distinct peak

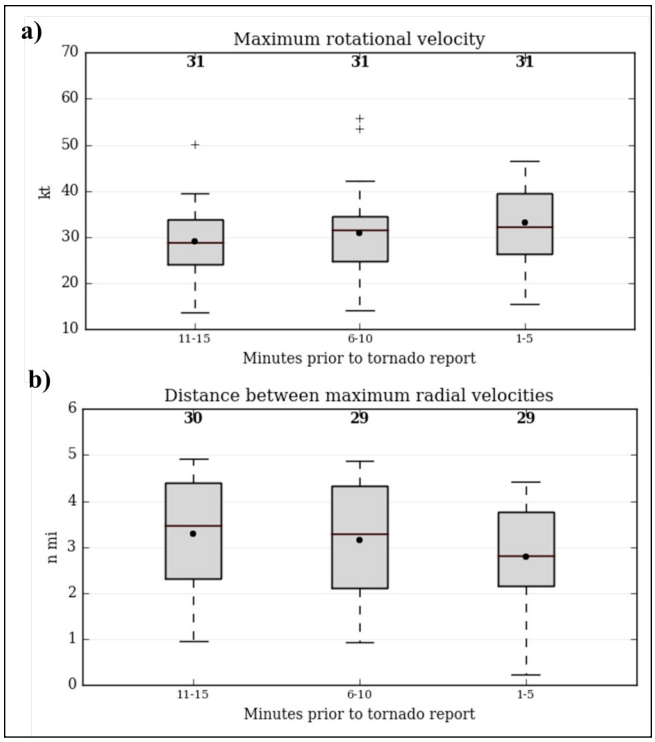

Figure 8. (a) The maximum rotational velocity and (b) the distance between the maximum inbound and outbound radial velocities from three scans (~11–15 min) to one scan (~1–5 min) prior to the initial tornado report for LMV QLCS tornadoes. Box-and-whisker plot conventions follow those described in Fig. 2.

occurring in March and April similar to adjacent regions within the United States. Seasonal differences are most apparent in QLCS tornado environments during the fall, with typical environments characterized by richer tropospheric moisture but weaker midlevel lapse rates when compared to winter and spring.

Based on a limited sample size, peak rotational velocity trends show a general increase in magnitude, and slight decrease in distance between maximum radial velocities when comparing EF0 and EF1+ LMV QLCS tornadoes. Of particular note, a temporal decrease occurs in the distance between the maximum radial velocities across the radar-identified mesovortex prior to tornadogenesis, as shown in Fig. 8b. Although the sample size is small, this result suggests that a contraction of the radar-identified circulation associated with the eventual tornado occurs prior to tornadogenesis in some cases, consistent with other radar-based studies (e.g., Ziegler et al. 2001). The information provided in Figs. 8 and 9 may be useful for meteorologists by providing an observed range of rotational velocities and distance between peak velocities for application in an operational warning setting, especially given the inherent difficulties in detecting the onset of QLCS tornadoes. Additional work, including the development of statistical analyses corresponding to larger sample sizes, would be necessary to substantiate the results and their physical implications.

Future work on this topic may involve including a larger sample size of LMV QLCS tornadoes for comparison with tornadoes from the rest of the CONUS. Also, additional work could be performed to investigate daytime versus nighttime variability of parameters representing LMV QLCS tornadoes, in addition to within-region variability of these tornadoes. Investigation and comparison with null events also could shed additional light on the predictability of LMV QLCS tornado environments. Further investigation of rotational velocity trends prior to the initial tornado occurrence, including an analysis of null events, may provide additional improvements in operational warning awareness in detecting QLCS tornadoes across the LMV.

Acknowledgments. The authors thank Andy Dean (SPC) for retrieval of data used in this study and to Israel Jirak (SPC) for review of this work. The authors also appreciate beneficial reviews of this manuscript from two anonymous reviewers, which greatly improved the quality of this work.

REFERENCES

Ashley, W. S., 2007: Spatial and temporal analysis of tornado fatalities in the United States: 1880–2005. *Wea. Forecasting*, **22**, 1214–1228, Crossref.

Bothwell, P. D., J. A. Hart, and R. L. Thompson, 2002: An integrated three-dimensional objective analysis scheme in use at the Storm Prediction Center. Preprints, *21st Conf. on Severe Local Storms/19th Conf. on Weather Analysis and Forecasting/15th Conf. on Numerical Weather Prediction*, San Antonio, TX, Amer. Meteor. Soc., JP3.1. [Available online at ams.confex.com/ams/pdfpapers/47482.pdf.]

Branick, M. L., F. Vitale, C.-C. Lai, and L. F. Bosart, 1988: The synoptic and subsynoptic structure of a long-lived severe convective system. Mon. *Wea. Rev.*, **116**, 1335–1370, Crossref.

Browning, K. A., 1986: Conceptual models of precipitation systems. *Wea. Forecasting*, **1**, 23–41, Crossref.

Cohen, A. E., S. M. Cavallo, M. C. Coniglio, and H. E. Brooks, 2015: A review of planetary boundary layer

parameterization schemes and their sensitivity in simulating southeastern U. S. cold season severe weather environments. *Wea. Forecasting*, **30**, 591–612, Crossref.

Davis, J. M., and M. D. Parker, 2014: Radar climatology of tornadic and nontornadic vortices in high-shear, low-CAPE environments in the mid-Atlantic and southeastern United States. *Wea. Forecasting*, **29**, 828–853, Crossref.

Gagan, J. P., A. E. Gerard, and J. Gordon, 2010: A historical and statistical comparison of "Tornado Alley" to "Dixie Alley." *Natl. Wea. Dig.*, **34** (2), 145–155. [Available online at nwafiles.nwas.org/digest/papers/2010/Vol34No2/Pg145-Gagan-etal.pdf.]

Guyer, J. L., and A. R. Dean, 2010: Tornadoes within weak CAPE environments across the continental United States. Preprints, *25th Conf. on Severe Local Storms*, Denver, CO, Amer. Meteor. Soc., 1.5. [Available online at ams.confex.com/ams/pdfpapers/175725.pdf.]

____, and I. L. Jirak, 2014: The utility of storm-scale ensemble forecasts of cool season severe weather events from the SPC perspective. Preprints, *27th Conf. on Severe Local Storms*, Madison, WI, Amer. Meteor. Soc., 37. [Available online at ams.confex.com/ams/27SLS/webprogram/Manuscript/Paper254640/27SLS%20Guyer%20Jirak%20SPC%20Cool%20Season%20CAMs.pdf.]

Hart, J. A., and A. E. Cohen, 2016a: The challenge of forecasting significant tornadoes from June to October using convective parameters. *Wea. Forecasting*, **31**, 2075-2084, Crossref.

____, and A. E. Cohen, 2016b: The statistical severe convective risk assessment model. *Wea. Forecasting*, **31**, 1697–1714, Crossref.

Przybylinski, R. W., J. Sieveking, and G. Schmocker, cited 2013: Classification of quasi-linear convective systems (QLCS) (including embedded bow echoes within QLCSs) and mesovortex characteristics across WFO St. Louis county warning area (CWA) and surrounding CWAs. [Available online at www.weather.gov/lsx/qlcslatest.]

Rogers, J. W., R. L. Thompson, and P. T. Marsh, 2014: Potential applications of a CONUS sounding climatology developed at the Storm Prediction Center. Preprints, *27th Conf. on Severe Local Storms*, Madison, WI, Amer. Meteor. Soc., P10.145. [Available online at ams.confex.com/ams/27SLS/webprogram/Manuscript/Paper255385/Extended%20abstract.pdf.]

Schaumann, J. S., and R. W. Przybylinski, 2012: Operational application of 0–3 km bulk shear vectors in assessing QLCS mesovortex and tornado potential. Preprints, *26th Conf. on Severe Local Storms*, Nashville, TN, Amer. Meteor. Soc., P9.10. [Available online at ams.confex.com/ams/26SLS/webprogram/Manuscript/Paper212008/SchaumannSLS2012_P142.pdf.]

Smith, B. T., R. L. Thompson, J. S. Grams, C. Broyles, and H. E. Brooks, 2012: Convective modes for significant severe thunderstorms in the contiguous United States. Part I: Storm classification and climatology. *Wea. Forecasting*, **27**, 1114–1135, Crossref.

____, ____, A. R. Dean, and P. T. Marsh, 2015: Diagnosing the conditional probability of tornado damage rating using environmental and radar attributes. *Wea. Forecasting*, **30**, 914–932, Crossref.

Thompson, R. L., B. T. Smith, J. S. Grams, A. R. Dean, and C. Broyles, 2012: Convective modes for significant severe thunderstorms in the contiguous United States. Part II: Supercell and QLCS tornado environments. *Wea. Forecasting*, **27**, 1136–1154, Crossref.

____, ____, A. R. Dean, and P. T. Marsh, 2013: Spatial distributions of tornadic near-storm environments by convective mode. *Electronic J. Severe Storms Meteor.*, **8** (5), 1–22. [Available online at ejssm.org/ojs/index.php/ejssm/article/view/125/93.]

Trapp, R. J., S. A. Tessendorf, E. S. Godfrey, and H. E. Brooks, 2005: Tornadoes from squall lines and bow echoes. Part 1: Climatological distribution. *Wea. Forecasting*, **20**, 23–34, Crossref.

Ziegler, C. L., E. N. Rasmussen, T. R. Shepherd, 2001: The evolution of low-level rotation in the 29 May 1994. Newcastle-Graham, Texas, storm complex during VORTEX. *Mon. Wea. Rev.*, **129**, 1339–1368, Crossref.